Theory and experiments based on tracked moving flexible DOE loops for speckle suppression in compact laser projection

Article *in* Optics and Lasers in Engineering · January 2020

DOI: 10.1016/j.optlaseng.2019.105845

CITATIONS
0

READS
23

9 authors, including:

Zichun Le
Zhejiang University of Technology
149 PUBLICATIONS **250** CITATIONS
SEE PROFILE

Anatoliy Lapchuk
National Academy of Sciences of Ukraine
69 PUBLICATIONS **367** CITATIONS
SEE PROFILE

I. V. Gorbov
Institute for Information Recording of NAS of Ukraine
23 PUBLICATIONS **28** CITATIONS
SEE PROFILE

A. V. Prygun
Institute for Information Recording of NAS of Ukraine
15 PUBLICATIONS **28** CITATIONS
SEE PROFILE

Optics and Lasers in Engineering 124 (2020) 105845

Contents lists available at ScienceDirect

Optics and Lasers in Engineering

journal homepage: www.elsevier.com/locate/optlaseng

Theory and experiments based on tracked moving flexible DOE loops for speckle suppression in compact laser projection

Zichun Le[a,*], A. Lapchuk[b], I. Gorbov[b], Zhiyi Lu[a], Songlong Yao[a], I. Kosyak[b], T. Kliuieva[b], Yanyu Guo[a], O. Prygun[b]

[a] College of Science, Zhejiang University of Technology, Hangzhou 310023, China
[b] Institute for Information Recording of NAS of Ukraine, Shpak Str. 2, Kiev 03113, Ukraine

ARTICLE INFO

Keywords:
Flexible DOE loop
Tracked motion
Speckle suppression

ABSTRACT

This paper describes a speckle suppression method using flexible diffractive optical elements (DOEs) based on binary random sequences with tracked motion. The DOE loops consist of 1D random-sequence diffractive structures with similar but different inclination angles. A mathematical approach for determining the optimal inclination angles and DOE speed for speckle suppression is developed, and a model for calculating the speckle suppression efficiency is constructed. Theoretical and experimental results show that the proposed method decreases the speckle contrast to below the sensitivity of the human eye, making it suitable for compact laser projections. The experimental results also indicate that current DOE production technology should be improved to avoid limiting the image quality.

1. Introduction

Laser diodes emit high-quality, optically efficient beams [1] from which high-color saturated images can be obtained [2]. Therefore, the use of lasers is very promising in the design of compact and energy-efficient projectors that produce high-quality color images [3–5]. However, laser images are strongly modulated by speckle, which significantly affects image quality [6]. The speckle contrast C is used to determine the speckle noise level:

$$C = \sigma / \bar{I} \tag{1}$$

where σ and $\bar{I}$ are the standard deviation of light intensity and the ensemble average light intensity, respectively. A highly efficient speckle suppression method is needed to decrease speckle noise to an acceptable level such that high-quality images can be produced. As the initial speckle level varies with the coherence of the laser, the final speckle contrast does not fully characterize the efficiency of the speckle suppression method. Therefore, to estimate the speckle suppression efficiency, a speckle suppression coefficient k is used:

$$k = C_0 / C \tag{2}$$

where C_0 and C denote the speckle contrast before and after the application of the speckle suppression method. Despite numerous studies on this topic, there is still no technical solution for speckle suppression that is sufficiently good for a compact laser projector system.

Speckle noise can be reduced by decreasing the temporal, spatial, or polarization coherence of laser beams [6]. Polarization decoherence can only decrease speckle noise by up to 30%, and can therefore only be used as a supplementary method [7]. Usually, lasers with large optical efficiency have a relatively small spectrum width (several nanometers) [1], which is not sufficient to decrease the speckle to below the sensitivity of the human eye [6]. It is possible to use temporal decoherence to obtain the spatial decoherence of a laser beam. An illuminating laser beam is divided into several beams with different optical paths by temporal decoherence, and these beams are then focused on one spot on the optical modulator plane to achieve angle diversity for speckle suppression [8,9]. However, the temporal decoherence of the laser beam makes it difficult to achieve sufficiently large decorrelated laser beams for suppressing speckle noise below the sensitivity of the human eye in a compact device.

Greater angle diversity, independent of laser beam coherence, can be achieved by using an active diffuser [10] or diffractive optical elements (DOEs) [11–20]. Active DOEs based on an electronically switching liquid crystal panel are an attractive concept, but the switching frequency speed is not large enough to be applied in laser projectors, although several research groups have recently obtained encouraging results [19,20]. The active diffusers or DOEs can also be fulfilled by mechanical movements, however, the speed of DOE movement must be sufficiently large that the human eye cannot detect the speckle contrast. A method of speckle suppression using DOEs on a plane vibrating substrate has been

* Corresponding author.
E-mail address: lzc@zjut.edu.cn (Z. Le).

https://doi.org/10.1016/j.optlaseng.2019.105845
Received 21 June 2019; Received in revised form 19 August 2019; Accepted 30 August 2019

proposed [10]. And a regular DOE structure based on a pseudorandom sequence has been proposed too for efficient speckle suppression [14–17]. In this case, a linear shift of the DOEs or rotation of quasi-spiral DOEs was proposed to achieve speckle suppression below the sensitivity of the human eye. However, practical realization in mobile projectors would require a large amplitude and vibration/shift/rotation speed to decrease the speckle contrast by a sufficient amount.

To date, the abovementioned methods have not demonstrated sufficient speckle suppression for use in compact devices such as pico-projectors. In a previous publication, we proposed a DOE loop based on pseudorandom sequences placed on a flexible film [18]. A DOE loop with tracked motion constructs a dynamic 2D DOE structure in real time by overlapping a double-sided moving 1D DOE, and its energy and volume requirements are very small. However, we did not achieve speckle suppression below the sensitivity of the human eye because of the suboptimal DOE parameters. The speckle suppression effect was significantly smaller than the expected value.

To fully develop and demonstrate an efficient technological solution for speckle suppression, which is suitable for the miniaturization of laser projectors, this paper reports a proposed theory for determining the optimal structure parameters of the DOE loop. The theory is further developed on the basis of our previous theoretical approach [15,16]. According to the proposed theory, speckle suppression effects are simulated with different DOE parameters, and the results are discussed in detail. An optical scheme for a compact laser projector is then constructed for speckle suppression experiments using RGB lasers. The experimental results indicate high speckle suppression efficiency, even when the DOE loops have suboptimal parameters. The further optimal parameters of the DOE loop, especially regarding the inclination angles and heights of the DOE components, are obtained on the basis of our theoretical and experimental results. The theoretical and experimental results in the present study demonstrate the possibility of obtaining very compact, highly energy efficient, and speckle-free laser pico-projectors.

2. Experimental setup

The specially designed flexible DOE loop is shown in Fig. 1. The flexible DOE loop consists of several parts, each of which is a binary 1D DOE structure based on a pseudorandom sequence with a different inclination angle φ_p close to $\pi/4$:

$$\varphi_p = \pi/4 + (p - p_0)\Delta\varphi \tag{3}$$

where p and p_0 are integers, $\Delta\varphi$ stands for the difference between inclination angles of two adjacent DOE parts and $\Delta\varphi \ll \pi/4$. In the present paper, we use a flexible DOE loop consisted of three parts of DOE structure with $p_0 = 2$ and $p = 1,\ 2,\ 3$. The DOE structure is a periodic 1D grating that is based on a binary pseudorandom sequence with code length $M = 15$. The DOE has an elementary cell of width T and a period length of $T_0 = MT$. The land and groove within DOE structure correspond to 1 and 0 in the binary sequence, respectively. The height of the structure is defined to give a half-wavelength shift in wavefronts passing through laser beams. The flexible DOE strip is rolled up in a loop; therefore, DOE structures on different sides of the loop have opposite inclination directions. The DOE loop is placed over two rotating poles, the rotation of which results in opposite directions of movement in DOE parts situated on different sides of the loop. This movement and the different inclination of different parts of the DOE results in field decorrelation of different diffraction orders. In a previous study [18], we did not determine the rigorous conditions for the optimal DOE inclination angle and DOE moving speed for decorrelation diffraction orders.

Fig. 2 illustrates the optical scheme of the proposed laser projector used in our experiments. In the Fig. 2, L_1 is the distance from DOE loop to objective lens, L_2 is the distance from objective lens to screen, L_3 is the distance from screen to camera lens, and L_4 is the distance from camera lens to photodiode array. And D_1 is the aperture of objective lens, D_2 is the aperture of camera lens. This is a simplified optical scheme for measuring speckle suppression efficiency, as it has no light beam homogenizer. The speckle suppression efficiency of our proposed method was measured without heterogeneity in the illuminated screen (detailed description is given in Section 5). To compare the image quality without and with speckle suppression, we used a transparent picture instead of an optical modulator in the experiments.

3. Theory of speckle suppression effect

Fig. 3 shows the generative process of dynamic 2D diffractive coding by means of a flexible DOE loop with tracked motion. The field of the heterogeneous laser beam that passes through the back side of the DOE loop can be presented as a set of fields of diffraction orders:

$$\begin{aligned} E &= \frac{A\sum_{n=-N}^{n=N} b_n exp\left(i\frac{2\pi n}{T_0}\left(v - tV\cos\left(\pi/4 + \Delta\varphi_1\right)\right)\right).}{\sum_{m=-N}^{m=N} a_m exp\left(i\frac{2\pi m}{T_0}\left(u + tV\cos\left(\pi/4 + \Delta\varphi_2\right)\right)\right)} \\ E^* &= \frac{A^*\sum_{n_1=-N}^{n_1=N} b_{n_1}^* exp\left(i\frac{2\pi n_1}{T_0}\left(v - tV\cos\left(\pi/4 + \Delta\varphi_1\right)\right)\right).}{\sum_{m_1=-N}^{m_1=N} a_{m_1}^* exp\left(i\frac{2\pi m_1}{T_0}\left(u + tV\cos\left(\pi/4 + \Delta\varphi_2\right)\right)\right)} \end{aligned} \tag{4}$$

where asterisks denote the complex conjugation, b_n and a_m are the amplitudes (relative to the amplitude of the incident beam) of the diffraction orders of 1D DOE structures on the front and back sides of the flexible DOE loop, respectively. A is the amplitude of the incident beam, n and m are the numbers of diffraction orders in different diffraction planes on the front and back sides of the DOE loop, respectively, and N denotes the number of diffraction orders that pass through the objective lens and are used in the speckle suppression mechanism. t denotes the integrated time and V is the speed of the tracked motion of the DOE loop. x and y denote the coordinates of Cartesian system, v and u are the coordinates of a point on the surface of the DOE loop in a nonorthogonal coordinate system, where the v and u axes are orthogonal to the

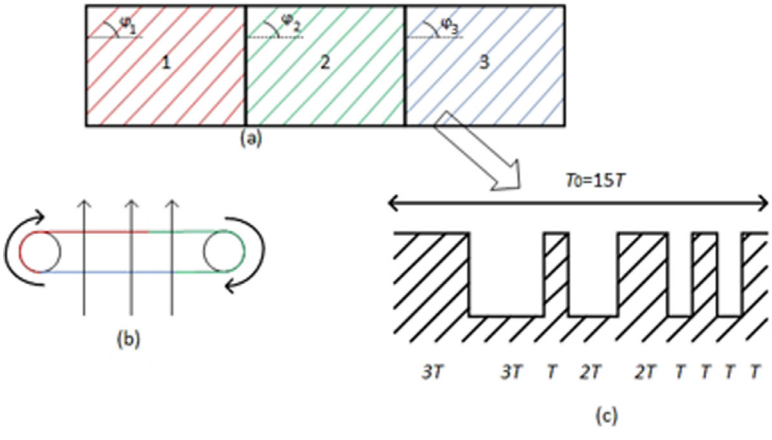

Fig. 1. Diagram of a flexible DOE loop consisting of three 1D DOEs with different inclination angles φ_p. Each part of the DOE loop is based on a binary pseudorandom sequence with code length $M = 15$. (a) structure of DOE loop; (b) flexible DOE loop on two rotation spindles; (c) structure of one DOE period.

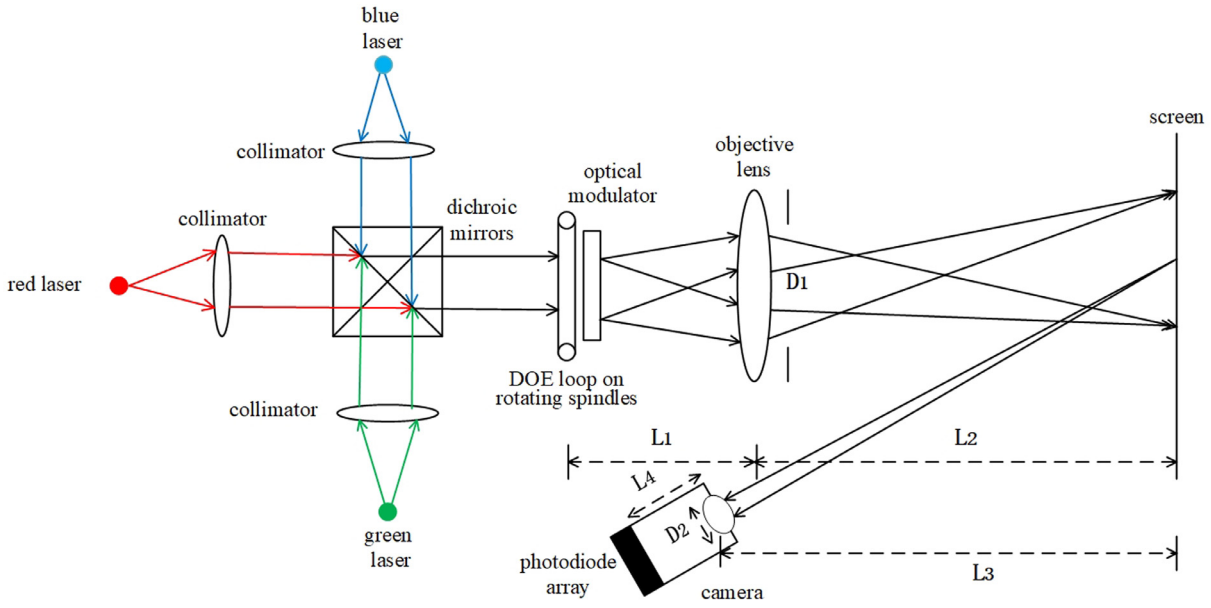

Fig. 2. Optical scheme used in experimental setup for speckle suppression efficiency measurement of the proposed method.

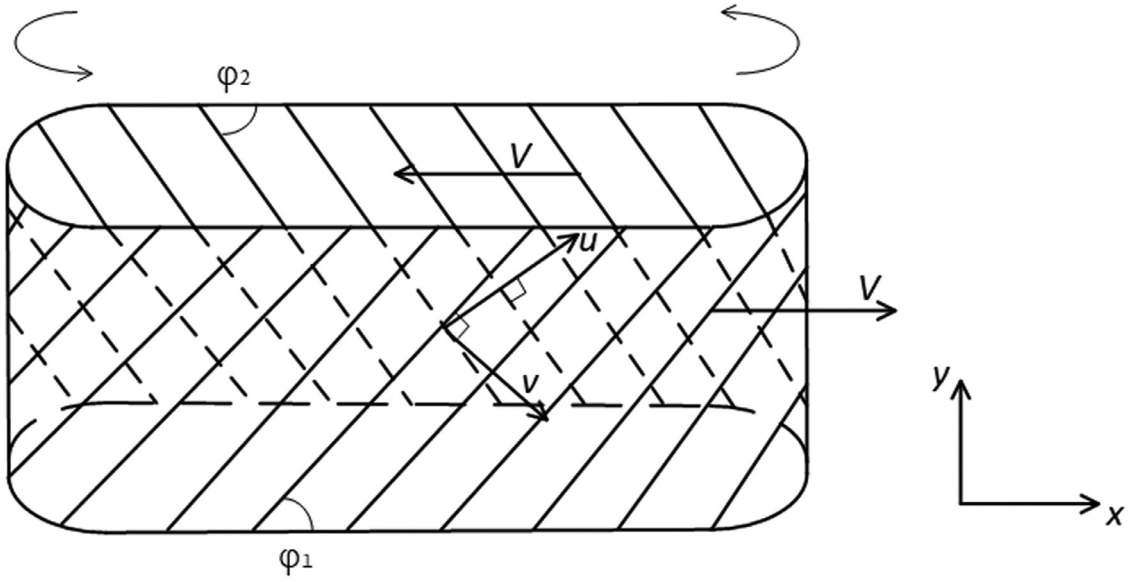

Fig. 3. Flexible DOE loop with tracked motion and nonorthogonal coordinate system (v, u). v and u are directed orthogonal to the edges of the 1D DOE structure on opposite sides of the DOE loop. x and y denote the coordinates of Cartesian system, V is the speed of the tracked motion of DOE loop along x axis.

edges of the front and back of the 1D DOE structure, respectively. The coordinates v and u can be calculated from the coordinates x and y using the following formula:

$$\begin{aligned} x &= v\sin\varphi_1 + u\sin\varphi_2;\ v = \frac{x\cos\varphi_2 - y\sin\varphi_2}{\sin(\varphi_1+\varphi_2)} \\ y &= -v\cos\varphi_1 + u\cos\varphi_2;\ u = \frac{x\cos\varphi_1 + y\sin\varphi_1}{\sin(\varphi_1+\varphi_2)} \end{aligned} \tag{5}$$

Using Eq. (4), the field intensity of a laser beam integrated over all light intensities for time Δt can be written as follows:

$$I(v,u) = |A|^2 \sum_{n,m,n_1,m_1=-N}^{n,m,n_1,m_1=N} b_n a_m b_{n_1}^* a_{m_1}^* exp\left(i\frac{2\pi v}{T_0}(n-n_1)\right) exp\left(i\frac{2\pi u}{T_0}(m-m_1)\right)$$

$$\int_{t=0}^{\Delta t} exp\left(i\frac{2\pi(n-n_1)}{T_0}tV\cos(\pi/4+\Delta\varphi_1)\right) exp\left(i\frac{2\pi(m-m_1)}{T_0}tV\cos(\pi/4+\Delta\varphi_2)\right)dt \tag{6}$$

where the summation is limited to the number of diffraction orders that passed through the objective lens and are used in the speckle suppression mechanism, and the integral is taken over the intensity integration time.

Considering the decorrelation of diffraction orders, the light intensity measured during the intensity integration time is just the sum of the intensities of the diffraction orders. Thus, all cross-diffraction-order terms in Eq. (6) should be equal to zero. As the integration in Eq. (6) contains exponential functions describing the decorrelation of fields of two diffraction orders, the phase shift of the exponent in the cross terms from

the initial to final point is then a nonzero integer multiple of 2π. This condition can be written as follows:

$$\frac{2\pi(n-n_1)}{T_0}\Delta tV\cos(\pi/4+\Delta\varphi_1)+\frac{2\pi(m-m_1)}{T_0}\Delta tV\cos(\pi/4+\Delta\varphi_2)=2\pi l \tag{7}$$

where l is a nonzero integer if $n\neq n_1$ or $m\neq m_1$. By using the notation of $\Delta tV = S$, where S is the DOE shift during the intensity integration time, we can rewrite Eq. (7) as follows:

$$(n-n_1)S\cos(\pi/4+\Delta\varphi_1)+(m-m_1)S\cos(\pi/4+\Delta\varphi_2)=lT_0 \tag{8}$$

Using the expression

$$\cos(\pi/4+\Delta\varphi_1)=\cos\pi/4\cos\Delta\varphi_1-\sin\pi/4\sin\Delta\varphi_1\approx\sqrt{2}/2(1-\sin\Delta\varphi_1) \tag{9}$$

Eq. (8) can be rewritten as

$$S'\left[(n-n_1)(1-\sin\Delta\varphi_1)+(m-m_1)(1-\sin\Delta\varphi_2)\right]=lT_0 \tag{10}$$

where $S'=\frac{\sqrt{2}}{2}S$ is approximately equal to the DOE shift in the v and u directions. The linearization of Eq. (10) should be valid with $l\neq 0$ for all decorrelated diffraction orders. We assume that $S'=N_0T_0$, $\sin\Delta\varphi_1=i/N_0$, $\sin\Delta\varphi_2=j/N_0$, where N_0 is the number of DOE periods shifted in the x direction during the whole integration time and i, j are integers denoting the DOE periods shifted in the y direction for DOE parts with inclination angles φ_1, φ_2, respectively. Eq. (10) can then be transformed into the Diophantine equation

$$N_0(n-n_1+m-m_1)-(n-n_1)i-(m-m_1)j=l \tag{11}$$

This Diophantine equation has a solution for any set of m, m_1, n, n_1 with a suitable choice of l. However, if we wish to decorrelate the field of diffraction orders in the range -N to N, we must identify the condition whereby all solutions of the Diophantine equation for that range do not have a solution with $l=0$. As a solution of a Diophantine equation is critically sensitive to the value of all coefficients, we must determine all the structure parameters of the DOE parts. In the following, we assume that the DOE has three parts with different inclination angles of $\varphi_1=\pi/4-\Delta\varphi$, $\varphi_2=\pi/4$, $\varphi_3=\pi/4+\Delta\varphi$. In this case, we seek the condition for which the solution of Eq. (11) has no solution with $l=0$ for sets of i and j including (1) $i=1$, $j=0$; (2) $i=0$, $j=1$; (3) $i=0$, $j=-1$; (4) $i=-1$, $j=0$; (5) $i=1$, $j=-1$; (6) $i=-1$, $j=1$ for diffraction orders ranging from $-N$ to N. Sets with the same value of i and j are not considered because it is assumed that the light spot never illuminates DOEs with the same inclination angle on both sides of the DOE loop (this case has no solution for the decorrelation of all diffraction orders and should be avoided). In addition, the DOE structure is designed in such a way that only the DOE areas close to the rotation spindle, which are outside of the light spot, can have the same DOE structure on opposite sides of the DOE loop. According to the assumptions above, we can determine the diffraction order decorrelation conditions for all possible sets of DOE parts.

Substituting the six sets of i and j values and $l=0$ into Eq. (11), we obtain:

$$\begin{aligned} &i=1,\ j=0, l=0,\ \frac{m-m_1}{n-n_1}=-\frac{N_0-1}{N_0}\\ &i=0, j=1, l=0,\ \frac{m-m_1}{n-n_1}=-\frac{N_0}{N_0-1} \end{aligned} \tag{12}$$

$$\begin{aligned} &i=0,\ j=-1, l=0,\ \frac{m-m_1}{n-n_1}=-\frac{N_0}{N_0+1}\\ &i=-1, j=0, l=0,\ \frac{m-m_1}{n-n_1}=-\frac{N_0+1}{N_0} \end{aligned} \tag{13}$$

$$\begin{aligned} &i=1,\ j=-1, l=0,\ \frac{m-m_1}{n-n_1}=-\frac{N_0-1}{N_0+1}\\ &i=-1, j=1, l=0,\ \frac{m-m_1}{n-n_1}=-\frac{N_0+1}{N_0-1} \end{aligned} \tag{14}$$

For Eq. (12), as (N_0-1) and N_0 have no common divisors, there will be no integer solution for n, n_1, m, m_1 in the range $-N$ to N if the absolute values of the denominator and numerator on the left-hand side do not exceed the denominator and numerator on the right-hand side, respectively. This condition can be written as follows:

$$N_0>2N+1 \tag{15}$$

Similarly, Eq. (13) has no integer solution for n, n_1, m, m_1 in the range $-N$ to N if the absolute value of the difference in the numerator and denominator on the left-hand side of Eq. (13) does not exceed the numerator and denominator on the right-hand side, respectively. This condition can be written as follows:

$$N_0>2N \tag{16}$$

Eq. (14) has no integer solution for n, n_1, m, m_1 in the range $-N$ to N if $(N_0-1)>2N$ and N_0 is an even number. This condition can be written as

$$N_0\geq 2(N+1),\ \text{and } N_0 \text{ is an even number} \tag{17}$$

During the rotation of the DOE loop, we can obtain all possible combinations of dynamic DOE codes on opposite sides of the DOE loop, as described above. Therefore, N_0 should satisfy all of the conditions obtained above, as described by Eq. (17).

It is reasonable to assume that N is equal to the length M of the pseudorandom binary code, as the main part of the energy of diffracted beams on the DOEs is distributed between the first $-M$ to M diffraction orders. As we have used a DOE structure based on a sequence of length $M=15$, we can calculate the required DOE inclination angles $\Delta\varphi$ of different parts of the DOE loop and minimize the DOE shift S required for the maximum speckle suppression effect.

$$\begin{aligned} &N_0=2(N+1)=2\times(15+1)=32\\ &\Delta\varphi=\sin^{-1}(1/N_0)=\sin^{-1}(1/32)=1.79^\circ\\ &S=\tfrac{2}{\sqrt{2}}S'=\sqrt{2}N_0T_0=2\sqrt{2}(N+1)T_0=2.7mm \end{aligned} \tag{18}$$

In the experiments, we used DOEs with a smaller difference in inclination angle of $\Delta\varphi=1^\circ$, which approximately corresponds to $N_0=58$. For this case, the DOE shift during one camera shot should be at least $S=\sqrt{2}N_0T_0=4.92\ mm$.

4. Simulations of speckle suppression effect

In Section 3, we determined the optimal parameters, including the DOE shift and inclination angles of DOE parts, for obtaining the best speckle suppression effect. However, for practical purposes, it is very important to know the sensitivity of the speckle suppression effect with respect to deviations from the optimal parameter values. To this end, we assume that the projector has an ideal objective lens that gives a magnified on-screen field distribution that is the same as the field just after the DOEs. Therefore, we can write the complex amplitude of the on-screen field as:

$$E_1(v,u,t)=E_0R(v-tV\cos(\pi/4+\Delta\varphi_1))R(u+tV\cos(\pi/4+\Delta\varphi_2)) \tag{19}$$

where $R(x)$ takes values of 1 and $\exp(ikh(n_{\text{index}}-1))$ for the land and grooves of the DOE structure, respectively. $k=2\pi/\lambda$ is the wave number, h is the DOE structure height, and n_{index} is the refractive index of the DOE material. The on-screen autocorrelation function for a DOE shift of length S can be calculated as:

$$\begin{aligned} A_1(v,u,v+\Delta v,u+\Delta u,S)=&\int_0^S|E_0|^2R(v-s\cos(\pi/4+\Delta\varphi_1))\\ &R^*(v+\Delta v-s\cos(\pi/4+\Delta\varphi_1))R(u+s\cos(\pi/4+\Delta\varphi_2))\\ &R^*(u+\Delta u+s\cos(\pi/4+\Delta\varphi_2))ds \end{aligned} \tag{20}$$

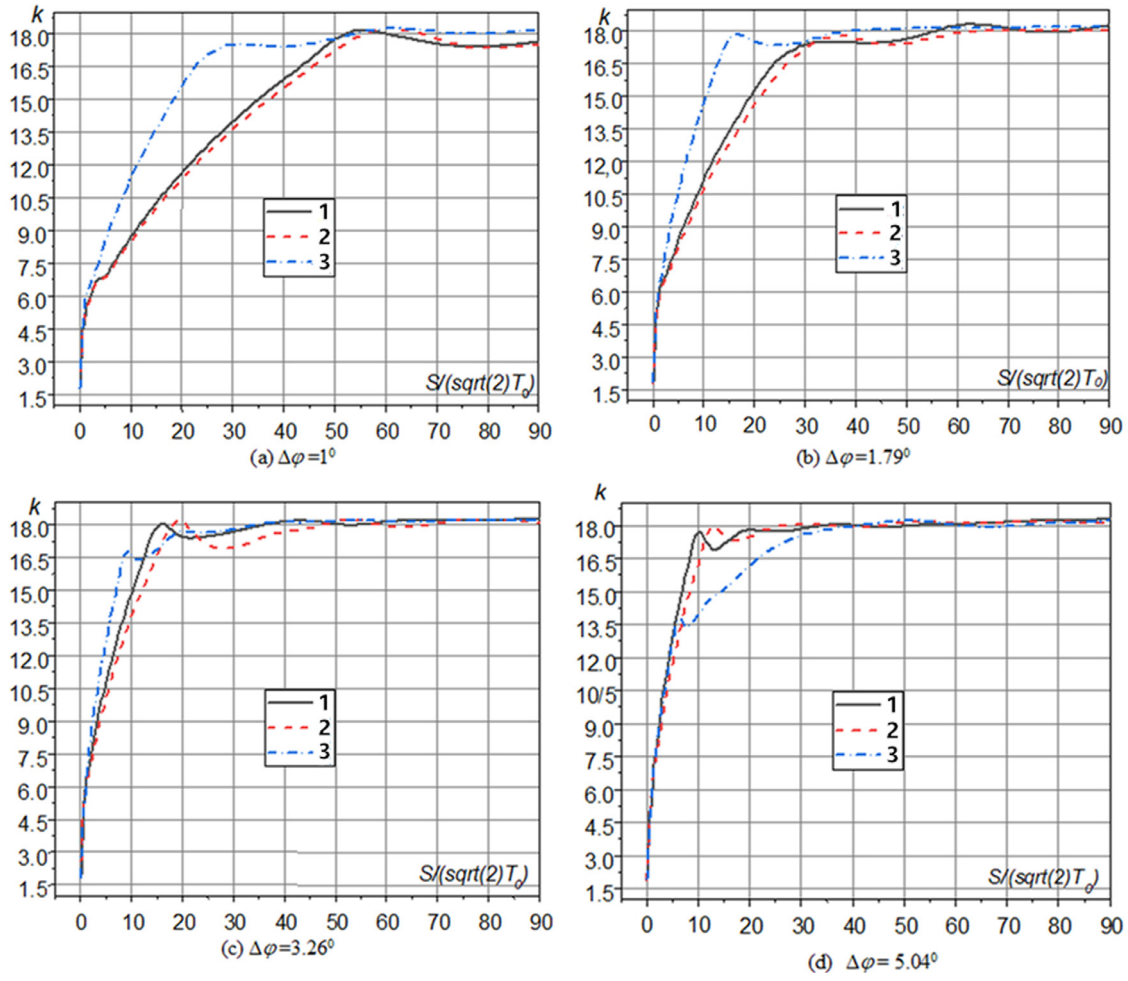

Fig. 4. Dependence of speckle suppression coefficient on DOE speed during intensity integration time for M-sequence-based DOE loop with a code length of $M = 15$. As DOE speed is related with DOE shift, the horizontal axis accordingly denote by $N_0 = S/(\sqrt{2}T_0)$. Curves 1, 2, 3 show 2D dynamic coding based on 1D DOE parts with difference inclination angles. curve 1: between $\varphi_1 = 45° + \Delta\varphi$ and $\varphi_2 = 45°$; curve 2: between $\varphi_1 = 45° - \Delta\varphi$ and $\varphi_2 = 45°$; curve 3: between $\varphi_1 = 45° - \Delta\varphi$ and $\varphi_2 = 45° + \Delta\varphi$.

Following Ref. [15], we obtain the speckle contrast as:

$$C = \sqrt{\frac{\int_0^{\infty}\int_0^{\infty} dvdu \int_0^{S'}\int_0^{S'} |A(v,u,v+\Delta v,u+\Delta u,S)|^2 \mathrm{sinc}^2\left[\frac{2\pi}{R_e}x(v,u)\right]\mathrm{sinc}^2\left[\frac{2\pi}{R_e}y(v,u)\right]\cdot \mathrm{sinc}^2\left[\frac{2\pi}{R_e}(x(v,u)+\Delta x(\Delta v,\Delta u))\right]\mathrm{sinc}^2\left[\frac{2\pi}{R_e}(y(v,u)+\Delta y(\Delta v,\Delta u))\right] d\Delta v d\Delta u}{\left(\int_0^{\infty}\int_0^{\infty} |A(x,y;x,y)|^2 \mathrm{sinc}^2\left[\frac{2\pi}{R_e}x(v,u)\right]\mathrm{sinc}^2\left[\frac{2\pi}{R_e}y(v,u)\right] dvdu\right)^2}} \tag{21}$$

where R_e denotes the spatial resolution (of the eye or photo camera) on the optical modulator plane. Eq. (21) is used to calculate the speckle suppression coefficient of our proposed method. We assume that the DOEs are fabricated on polypropylene film with a refractive index of $n_{\mathrm{index}} = 1.49$. Fig. 4 shows the dependence of the speckle suppression coefficient on the DOE shift S during the intensity integration time for DOEs with various differences in inclination angle $\Delta\varphi$. As the DOE moving speed V is related to the DOE shift S ($S = tV$), Fig. 4 actually shows the dependence of the speckle suppression coefficient on the DOE speed. In the developed flexible DOE loop, laser beam passes through a 2D dynamic coding based on two different 1D DOE parts in different time due to DOE shift. In Fig. 4, curves 1, 2, 3 indicate the speckle suppression coefficient for the case when laser beam passes through the 2D dynamic coding by overlapping of the two different 1D DOE parts. The curve 1 stands for the case when the overlapping occurs between 2nd and 3rd 1D DOE parts, the curve 2 stands for the case of overlapping between 1st and 2nd 1D DOE parts and curve 3 stands for the case of overlapping between 1st and 3rd 1D DOE parts (see Eq. (3) and Fig. 1). For $\Delta\varphi = 1°$ and $\Delta\varphi = 1.79°$ (see Fig. 4(a) and (b)), the speckle suppression efficiency increases with DOE speed and reaches a maximum at the exact DOE shift suggested by the above estimation (with a suitable value of N_0). For further increase of DOE speed from optimal value, the difference between initial and final phase of the field of different diffraction order will be changed and the exact decorrelation between diffraction orders will be lost. Therefore, the speckle suppression efficiency decreases slightly. With a continuous increase in DOE speed, the next full decorrelation (it is possible even for more diffraction orders) and the next efficiency maximum can be obtained. However, the variation of speckle suppression efficiency between two maximums is small since only partial correlation between diffraction orders can be obtained with the increase of DOE speed. And the value of the possible partial correlation decreases with the increase of DOE speed. Therefore, the speckle contrast is almost constant after reaching the optimal DOE shift.

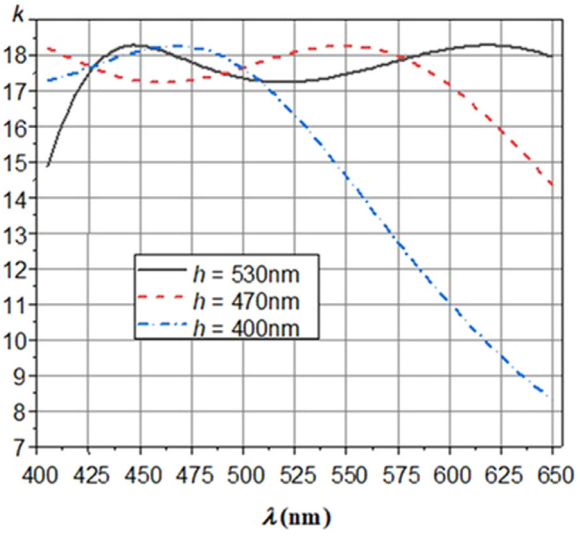

Fig. 5. Dependence of the speckle suppression coefficient on laser wavelengths for M-sequence-based DOE loop with a code length of $M=15$. $\Delta\varphi = 1°$, $S = 4.92$mm, $\varphi_1 = 46°$, $\varphi_2 = 45°$

For a larger inclination angle difference of $\Delta\varphi = 3.26°$ (see Fig. 4(c)), the maximum speckle suppression is obtained at a slightly different DOE speed for different DOE parts, although it can still be accurately evaluated using Eq. (18). Note that the maximum speckle suppression can be reached with the smallest DOE speed in this case. Increasing $\Delta\varphi$ to 5.04° (see Fig. 4(d)) results in a change in the dependence of the speckle suppression coefficient on the DOE shift for curve 3. In this case, a rather long DOE shift is needed to attain the maximum speckle suppression effect. Note that a shift of at least $2\sqrt{2}N_0T_0$ is required to achieve the maximum speckle suppression effect.

The numerical simulations have also shown that the speckle suppression efficiency is not sensitive to small changes of DOE speed and DOE inclination angles, when DOE speed and DOE inclination angle are closed to the optimized value. The large tolerance with optimized parameters is significant for the fabrication of DOE loop.

Fig. 5 shows the speckle suppression efficiency with respect to the laser wavelength for $\Delta\varphi = 1°$ and for different DOE structure heights of 530 nm, 470 nm, and 400 nm for the optimal DOE speed V (speed is measured by DOE shift). The simulation gives approximately the same speckle suppression efficiency $k = 17.75 \pm 0.5$ across the visible range 425 nm $< \lambda <$ 650 nm for a DOE structure height of 530 nm. However, for the two smaller DOE structure heights, the speckle suppression efficiency exhibits a significant drop at longer wavelengths.

5. Experimental results and discussion

The optical scheme for speckle suppression using the proposed method is shown in Fig. 2. In the experiments, we used three DOE loops, each having the same structure except for the structure height, which was 530 nm in DOE loop 1, 470 nm in DOE loop 2, and 400 nm in DOE loop 3. The DOEs were arranged on transparent polypropylene film with a refractive index of 1.49. Each DOE loop has three DOE parts with inclination angles of 44°, 45°, and 46° (hence $\Delta\varphi = 1°$). The DOE structure was based on a pseudorandom sequence with a code length of $M=15$. The DOE loops measured 75 mm long and 40 mm wide, and were made from DOE strips including the three DOE parts by gluing opposite ends using hot air heating. The DOE loops were placed on two spindles of diameter 4 mm. One spindle was connected to a motor controlling the DOE shift, and the other spindle was connected to a spring to pull the film containing the DOE structures. RGB laser diodes were used in experiments: blue laser $\lambda = 450$ nm, green laser $\lambda = 530$ nm, and red laser $\lambda = 638$ nm. The projective lens had a diameter of 50 mm and a focal length of 100 mm. The input camera aperture was 1 mm and the focal length of the camera objective was 25 mm. The distances from the DOE to the objective (L_1), from the objective to the screen (L_2), and from the screen to the camera (L_3) were 110 mm, 1200 mm, and 1310 mm, respectively. The distance from the camera aperture to the photodiode array matrix was $L_4 = 26$ mm, and the photodiode had a transverse size of 5.8 μm. DOE loops were produced on both thick (50 μm) and thin (25 μm) polypropylene films. Measurements were made for three speeds of DOE shift: 29 mm/s, 23.4 mm/s, and 16.7 mm/s. An image shot time of 0.2 s was used in the experiments. According to the simulations, a DOE shift of around 5.04 mm should ensure the maximum speckle suppression effect. The DOE shifts during camera shots were chosen as 5.8 mm, 4.7 mm, and 3.34 mm for the three DOE speeds of 29 mm/s, 23.4 mm/s, and 16.7 mm/s, respectively. The first speed produces a larger DOE shift than required, the second one gives a slightly smaller shift than required, and the third one gives a DOE shift that is 34% smaller than required. The experimental results are presented in Table 1.

From the data in Table 1, it is clear that DOE loop 1 (DL_1) and DOE loop 2 (DL_2) provide speckle suppression that is below the sensitivity

Table 1
Speckle suppression effect for different films, different DOE structure heights, and different DOE speeds, where F_{th} denotes the film thickness, DL denotes the number of DOE loops.

F_{th}	DL	V	$\lambda = 450$ nm			$\lambda = 530$ nm			$\lambda = 638$ nm		
			C_0	C	k	C_0	C	k	C_0	C	k
50 μm	DL_1	V_1	0.25	0.02	12.9	0.27	0.022	12.5	0.55	0.03	18.6
		V_2	0.25	0.02	12.6	0.27	0.022	12.4	0.55	0.033	16.7
		V_3	0.25	0.02	12.5	0.27	0.022	12.2	0.55	0.041	13.3
	DL_2	V_1	0.25	0.021	12.1	0.29	0.024	11.7	0.56	0.038	14.6
		V_2	0.25	0.021	12.0	0.29	0.023	12.3	0.56	0.039	14.3
		V_3	0.25	0.021	12.4	0.29	0.028	10.3	0.56	0.043	13.0
	DL_3	V_1	0.25	0.023	10.6	0.29	0.024	11.7	0.51	0.07	7.3
		V_2	0.25	0.022	11.2	0.29	0.025	11.6	0.51	0.075	6.9
		V_3	0.25	0.02	12.4	0.29	0.027	10.4	0.51	0.076	6.7
25 μm	DL_1	V_1	0.24	0.022	11.2	0.29	0.021	13.9	0.54	0.032	17.2
		V_2	0.24	0.021	11.8	0.29	0.021	13.4	0.54	0.035	15.8
		V_3	0.24	0.023	10.7	0.29	0.022	12.9	0.54	0.033	16.5
	DL_2	V_1	0.26	0.021	12.3	0.29	0.022	13.3	0.55	0.036	15.2
		V_2	0.26	0.02	12.9	0.29	0.021	13.4	0.55	0.035	15.6
		V_3	0.26	0.022	11.7	0.29	0.022	13.0	0.55	0.037	14.7
	DL_3	V_1	0.24	0.023	10.9	0.29	0.026	11.0	0.54	0.068	8.0
		V_2	0.24	0.021	11.8	0.29	0.026	11.1	0.54	0.068	8.1
		V_3	0.24	0.022	11.3	0.29	0.026	11.1	0.54	0.071	7.7

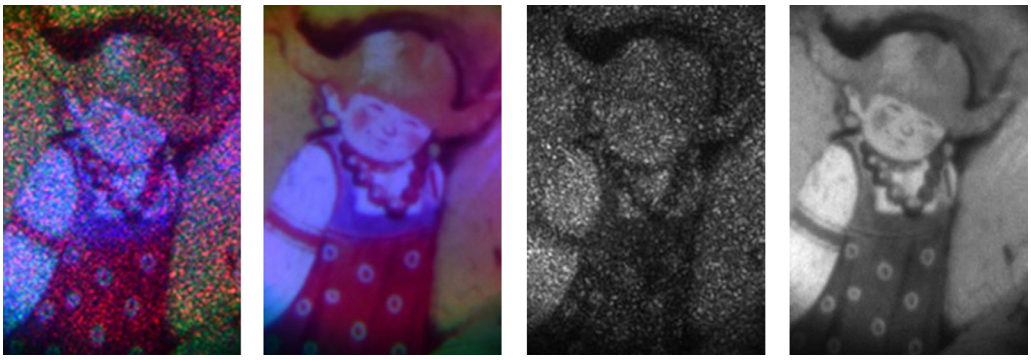

Fig. 6. Color images obtained without (a) and with (b) speckle suppression and grayscale images obtained without (c) and with (d) speckle suppression.

of the human eye over the entire visible range for all three DOE shift speeds. DOE loop 1 has a structure height of 530 nm, which provides a wavefront shift of half the wavelength in the middle of the waveband used in the experiments. Therefore, this is the optimal height for speckle suppression for the three RGB lasers, which is confirmed by the simulation results given above. In spite of the large shift in structure height from the optimal value of 60 nm, DOE loop 2 has approximately the same speckle suppression efficiency as DOE loop 1. This illustrates the advantage of our method for large-bandwidth, efficient speckle suppression, as the two sides of the two 1D DOEs are used for speckle suppression [17]. Even DOE loop 3, which has the optimal height for a laser with $\lambda = 416$ nm (beyond the operating wavelength range of RGB lasers in our experiments), exhibits good suppression efficiency for the red laser, $k \sim 7.3$ (we obtained $k \sim 8.7$ in the simulations, see Fig. 5).

The significant smaller speckle suppression effect was achieved in experiment than in simulation for green and blue lasers (see Fig. 5). We suppose the reasons are as follows. The images obtained in experiments had small diffraction fringes due to refraction from dichroic mirror with nonoptimal parameters. It causes additional variation of intensity on screen that make practically impossible to measure speckle contrast below 0.02. In addition, it results in the saturation of measured speckle suppression due to small initial speckle contrast of green and blue images. In order to verify our assumption, we made a further experiment by using the best three DOE loops with speed of 29 mm/s and removing the dichroic mirrors from optical scheme. The new laser diodes were used in the further experiment with initial speckle contrast C_0 in the range of 0.45–0.48 for red laser, 0.32–0.33 for green laser and 0.40–0.42 for blue laser. In this case, we obtained speckle suppression coefficient k as follows: 21.3 (red laser), 15.3 (green laser) and 20.9 (blue laser) for DOE loop 1; 19.9 (red laser), 14.9 (green laser) and 20.6 (blue laser) for DOE loop 2; 9.8 (red laser), 17.2 (green laser) and 21.1 (blue laser) for DOE loop 3. The results from further experiment show a good agreement with the simulation results. Because of the problem with DOE quality, we obtained different speckle contrast for different DOE sample. Therefore, the fabricating technology is still needed to be improved for making perfect DOE surface as well as the optical scheme with optimal components for speckle suppression.

To demonstrate the image quality before and after speckle suppression, we used color pictures on transparent film placed at the optical modulator plane to obtain color images on a screen. The image on the screen was taken by a grayscale camera and a color camera situated at the same place and having the same aperture size as in the experiments. The obtained pictures are shown in Fig. 6. One can observe that the speckle noise is practically invisible after speckle suppression, although the picture details are almost impossible to see before speckle suppression because of the speckles in both the color and grayscale images. Note that true color reproduction decreases from the center to the periphery of the picture. This is because the speed at which the light intensity decreases varies in different color beams, as there is no beam homogenizer in the optical scheme (see Fig. 2).

The above analysis indicates that a DOE shift of at least $2\sqrt{2}NT_0 = 2.55$mm during the intensity integration time is required. Projectors require at least 25 color pictures per second, with every color received at separate time intervals. Thus, a total of 75 pictures with different colors per second are needed. Therefore, the speed of the DOE shift should be at least $75 \times 2.55\,\text{mm}/s = 191.25\,\text{mm/s}$. To achieve smaller projectors and use smaller DOE speeds, a high numerical aperture lens must be used as the objective. For example, if an objective with a numerical aperture of 0.5 is used, one can decrease the DOE primitive cell size by a factor of three, from 4 μm to 1.3 μm, with a proportional decrease in the DOE speed to 63.75 mm/s. This DOE velocity is sufficiently low to be realized using our proposed method, but it is practically impossible for other methods with moving diffusers or DOEs, such as DOE vibration, to reach such speeds.

6. Conclusion

To analyze and optimize the performance of our method based on a tracked moving DOE loop for speckle suppression, the underlying theory of the speckle suppression effect has been developed. This allowed us to design the optimal structure parameters of DOE loops. Analytical expressions for the optimal inclination angles of DOE parts and the optimal DOE speed to achieve the maximum speckle suppression effect were derived. Simulations and experimental results show that the proposed method allows one DOE loop to be used to suppress speckles across the entire range of visible light. Speckle contrast below 3% was obtained for red, green, and blue lasers, and color pictures without visible speckle were produced. The speed of the DOE shift and the size of the device needed for efficient speckle suppression are acceptable for application to portable laser projectors. The mathematical model and numerical simulations have shown that the optimal difference in inclination angles of different DOE parts should be at least twice that used in the present experiments to decrease the required DOE speed by a factor of two. The experimental results show that the technology used for DOE production is still not good enough to decrease variations in the intensity of the illumination beam to below 2%. The moving mechanism of DOE loop is also needed to be further improved because DOE structures were contacted with spindles in the present system. The friction will accelerate the degradation of DOE loop. In addition, a high-quality compact beam homogenizer is required pico-projector setups using the proposed speckle suppression mechanism.

Funding

This work was supported by National Natural Science Foundation of China [grant number 61975183]; Special Funding from the “Belt and Road” International Cooperation of Zhejiang Province [grant number 2015C04005]; R&D Funding from NAS of Ukraine [grant number 0114U002061].

References

[1] Sands D. Diode lasers. Taylor & Francis; 2004.
[2] Buckley E. Pico-projection systems. Wiley; 2017.
[3] Trisnadi JI, Carlisle CB, Monteverde V. Overview and applications of grating light valve TM based optical write engines for high-speed digital imaging. Proc SPIE 2004;5348:52–64.
[4] Yun SK, Song J-H, Yeo I-J, Victor Y, An S-D, Park H-W, Yang H-S, Han K-B, Lee Y-C, Choi Y-J, Lee S-H, Oh M-S, Shin D-H, Kim J-S, Ryu S-W, Oh K-Y, Ko Y-J, Hong S-K, Park C-S, Yoon S-K, Jang J-W, Kyoung J-H, Hong Y-S, Kim C-C, Lim O-K, Lapchuk A, Lee J-K, Park D-H, Shin S-W, Kang J-C, Lee S-W, Kim S-K, Byun G-Y, Oh S-K, Lee J-S, Hwang Y-N, Kim D-W, Woo K-S, Kim E-J, Park C-W, Go C-D, Lee Y-J, Kim B-H, Kim C-H, Kim D-J, Park J-S. Spatial optical modulator (SOM): Samsung's light modulator for the next generation laser display. Proc. SPIE 2007;6487:648710.
[5] Freeman M, Champion M, Madhavan S. Scanned laser pico-projectors: seeing the big picture (with a small device). Opt Photonics News 2009;20(5):28–34.
[6] Goodman JW. Speckle phenomena in optics. Roberts & Company; 2006.
[7] Trisnadi JI. Speckle contrast reduction in laser projection displays. Proc SPIE 2002;4657:131–7.
[8] Manni JG, Goodman JW. Versatile method for achieving 1% speckle contrast in large-venue laser projection displays using a stationary multimode optical fiber. Opt Express 2012;20(10):11288–315.
[9] An S-D, Lapchuk A, Yurlov V, Song JH, Park HW, Jang JW, Shin WC, Kargapoltsev S, Yun S-K. Speckle suppression in laser display using several partially coherent beams. Opt Express 2009;17(1):92–103.
[10] Kubota S, Goodman JW. Very efficient speckle contrast reduction realized by moving diffuser device. Appl Opt 2010;49(23):4385–91.
[11] Wang L, Tschudi T, Halldórsson T, Pétursson PR. Speckle reduction in laser projection systems by diffractive optical elements. Appl Opt 1998;37(10):1770–1775.
[12] Trisnadi JI. Hadamard speckle contrast reduction. Opt Lett 2004;29(1):11–13.
[13] Pan J-W, Shih C-H. Speckle reduction and maintaining contrast in a laser pico-projector using a vibrating symmetric diffuser. Opt Express 2014;22(6):6464–6477.
[14] Nadeem Akram M, Kartashov V, Tong Z. Speckle reduction in line-scan laser projectors using binary phase codes. Opt Lett 2010;35(3):444–6.
[15] Lapchuk A, Kryuchyn A, Petrov V, Yurlov V, Klymenko V. Full speckle suppression in laser projectors using two Barker code-type diffractive optical elements. J Opt Soc Am A 2013;30(1):22–31.
[16] Lapchuk A, Prygun O, Fu M, Le Z, Xiong Q, Kryuchyn A. Dispersion of speckle suppression efficiency for binary DOE structures: spectral domain and coherent matrix approaches. Opt Express 2017;25(13):14575–97.
[17] Lapchuk A, Pashkevich G, Prygun O, Kosyak I, Fu M, Le Z, Kryuchyn A. Very efficient speckle suppression in the entire visible range by one two-sided diffractive optical element. Appl Opt 2017;56(5):1481–8.
[18] Lapchuk A, Gorbov I, Le Z, Xiong Q, Lu Z, Prygun O, Pankratova A. Experimental demonstration of a flexible DOE loop with wideband speckle suppression for laser pico-projectors. Opt Express 2018;26(20):26188–95.
[19] Ardasheva LI, Kundikova ND, Sadykova MO, Sadykov NR, Chernyakov VE. Speckle-pattern rotation in a few-mode optical fiber in a longitudinal magnetic field. Opt Spectr 2003;95(4):645–51.
[20] Andreev AA, Andreeva TB, Kompanets IN, Minchenko MV, Pozhidaev EP. Speckle-noise suppression due to a single ferroelectric liquid-crystal cell. J SID 2009;17(10):801–7.